Fire accident report verification using fire dynamics simulator: a case study from Chiayi City, Taiwan

Chun-Cheng Lai[1] · Chen-Rui Cao[1] · Chi-Min Shu[2,3]

Abstract

A fire dynamics simulator (FDS) and Smokeview 3D (SMV) were used to recreate a fire disaster that occurred in Chiayi City, Taiwan, on May 02, 2012. The two buildings involved were traditional wooden constructions; however, one was repaired, and the roof was rebuilt with asbestos shingles and iron sheets. This study sought to verify the existing fire accident report and witness statements. A summary of relevant literature on the topic was provided to determine the optimal settings for the simulation and shortlist other influential factors from the current relevant reports. Furthermore, relevant parameters, such as the total heat release rate was 3000 kW of the fire source, the fire growing factor was 0.188 kW s^{-2}, the mesh size parameters were 0.0–2.0 m on the x-axis, 0.0–5.0 m on the y-axis, and 0.0–5.0 m on the z-axis. Meanwhile, four different nominal sizes, namely 0.05, 0.1, 0.2, and 0.25, were also tested in the simulation to find the suitable simulation result when other parameter data were fixed and D^* was divided by the nominal size, 0.1, with 14.62 yielded at least. The simulation results were compared with the fire accident report and witness statements. The area presumed as the initial ignition place in which the fire commenced to advance between the two buildings was not considered in the original fire accident report, and the simulation showed that this was fair and reasonable.

Keywords Fire dynamics simulator · Smokeview · Wooden constructions · Fire accident report · Initial ignition place

List of symbols

α	Fire growth coefficient (kW s^{-2})
α	Significance level
Cm	Centimeter
C_p	Specific heat of the air (kJ $(kg\ K)^{-1}$)
D^*	Characteristic fire diameter (m)
Gb	Gigabit
GHz	Gigahertz
g	Gravitational acceleration (m s^{-2})
kW	Kilowatt
Mb	Megabit
m	Meter
n	Sample size
ρ_∞	Density of the air (kg m^{-3})
$\dot{Q}$	Heat release rate (kW)
s	Standard deviation for sample
s	Second
T_∞	Environment temperature (K)
t	Time (s)
t_o	Fire growth time (s)
μ	Population mean
δ_x	Nominal size (m)
$\bar{x}$	Sample mean
σ	Standard deviation for population
z	Random variable

Abbreviations

BFRL	Building and fire research laboratory
CI	Confidence interval
CPU	Central processing unit
CCTV	Closed circuit television
FDS	Fire dynamics simulator
HRR	Heat release rate (kW)
HRRPUA	Heat release rate per unit area (kW m^{-2})
LES	Large eddy simulation

✉ Chi-Min Shu
shucm@yuntech.edu.tw

1 Graduate School of Engineering Science and Technology, National Yunlin University of Science and Technology (YunTech), Yunlin 64002, Taiwan, ROC

2 Department of Safety, Health, and Environmental Engineering, YunTech, 123, University Rd., Sec. 3, Douliou 64002, Yunlin, Taiwan, ROC

3 Center for Process Safety and Industrial Disaster Prevention, Department and Graduate School of Safety, Health, and Environmental Engineering, YunTech, Yunlin 64002, Taiwan, ROC

NIST	National Institute of Standards and Technology
OBST	Obstruction
RAM	Random access memory
SMV	Smokeview
THCP	Thermocouple
TAU_Q	Time indicates that the heat release rate (HRRPUA), surface temperature (TMP_FRONT), and/or normal velocity (VEL, VOLUME_FLOW), or MASS_FLUX_TOTAL are to ramp up to their prescribed values in TAU seconds and remain there

Introduction

Because of seismic performance [1], mechanical strength, and sound hydrothermal comfort [2], wooden buildings were widely constructed in numerous countries and in many different areas. After the Japanese government colonized Taiwan from 1895 to 1945, many wooden structures remained for a long time, such as temples, shrines, and residences. Therefore, there are still many wooden buildings in Taiwan. In addition, this even seems an essential characteristic of the historical buildings of Taiwan. Typically, these wooden buildings and the timber have a high fire load and low fire resistance rating. They tend to be readily ignited by electrical sparks, arcs, hot objects, hot surfaces, friction, radiant heat, chemical reactions, and other unregulated heat sources and combust [3–5]. Moreover, when wooden buildings are on fire, wood-based materials undergo pyrolysis and charring, weakening mechanical properties and forming cracks [6–9]; the fire rapidly gathers momentum, which can result in casualties and further damage to surrounding properties [10].

At the beginning of a fire investigation, it is necessary to adopt a scientific approach, i.e., "the systematic pursuit of knowledge involving the recognition and formulation of a problem, the collection of data through observation and experiment, and the formulation and testing of a hypothesis" [11]. There are seven steps involved in this modern iterative process: to recognize the need, define the problem, collect data, analyze the data, develop a working hypothesis, test the working hypothesis, and reach conclusions or offer opinions [12].

Thus, before speculating on the origin and possible causes of a fire, fire investigators must carefully observe the burning conditions and collect the potential sources, such as those statements made by witnesses and residents and CCTV images, along with any other available data. Relatively complete data analysis is often sufficient to reveal a fire's origin, causes, or developmental path [12].

Yet, there are rare situations in which investigators are unable to conclusively determine the origin of a fire, because of some unique factors, such as prolonged combustion or some combustible object overload, leading to a large explosion that completely destroys the fire scene. In such events, even with a fully equipped laboratory, fire investigators may not be able to find the correct combustion traces or the evidence of residual ash they need.

As for indeterminate conditions, an alternative that was not made available in the past is now considered. Fire simulation programs, such as the fire dynamics simulator (FDS) and Smokeview (SMV), are powerful tools for modeling fire situations, to reveal useful data for fire investigators. These data can be compared to witness and resident statements and combined with combustion conditions and other available images to better validate the investigation into the cause of fire motivated by pure supposition.

On May 02, 2012, a severe fire broke out in Chiayi City, Taiwan. The roofs of those wooden buildings that were repaired and built of some partial asbestos shingles and iron sheets at an earlier time burst into flames. Fire investigators collected witness and resident statements about the flow of smoke from the upper floor of building B; interviewers described the sound of an explosion, from the direction of building B. There was no smoke or fire in building A early in the fire. CCTV equipment installed in building A showed that initially no fire or smoke had appeared on building A's second floor or stairway. Because of these statements and images, fire investigators concluded that the gap between buildings A and B was not the first ignition place.

Although there is still a possibility that the fire began in the gap between the two buildings, FDS can be used to investigate this possibility better. This study used FDS to reconstruct the 2012 fire disaster in Chiayi City, Taiwan, because this technique can provide valuable simulation data through which the initial fire location and smoke flow dynamics can be validated to ascertain whether this can remain consistent with the witness statements and the fire reports [13].

Fire report preliminary summary

Buildings A and B were fashion clothing shops and both caught fire on May 02, 2012 in Chiayi City, Taiwan. Furthermore, the ambient temperature was 302.95 K and the characters of these two buildings are described as follows [13].

Ambient environmental conditions

The ambient temperature and humidity were 302.95 K and 69%, respectively.

Characteristics of building A

This was a two-story wooden building that was partially covered with asbestos roof shingles and iron sheets, but the wall on the second floor, next to building B, was built of wood. The roof of this building was higher than that of building B by 28.0 cm. The distance between these two buildings on the second floor was 34.0 cm.

Characteristics of building B

It was a three-story wooden building that was also partially covered with asbestos roof shingles and iron sheets. The walls on the second and third floors closest to building A were made of asbestos roof shingle. From the ground, the height of the third floor was 520 cm.

Although both buildings were primarily wooden, parts were once repaired using asbestos roof shingles and iron sheets. Furthermore, the wall of building A was made of wood, whereas building B was made of asbestos roof shingles. In this research, the investigation was made explicitly into the distance measuring a 34.0 cm gap between the two buildings.

The statements about situations described by the witnesses and residents are as follows: The flow of smoke came out from the upper floor of building B. The sound of an explosion was heard from the direction of building B, but no smoke or fire was visible in building A at the early stage of the fire. Furthermore, the CCTV equipment installed in building A showed no fire or smoke on the second floor or stairway of building A in the initial stages until a power outage.

Accordingly, the above enabled the fire investigators not to consider the gap as a source of fire ignition, based on the witness and resident statements, the observed combustion conditions, and the CCTV images [13].

Computer simulation

Fire dynamics simulator (FDS)

FDS, a computational fluid dynamics model for fire-driven fluid flows, was cooperatively developed by the National Institute of Standards and Technology (NIST) and Building and Fire Research Laboratory (BFRL) [14]. By referring to the Navier–Stokes equation, the simulation can resolve a large eddy simulation (LES) and account for information related to fire speed and thermally driven flows. The emphasis is placed on smoke and heat transport from a fire source to better describe the fire evolution [15].

FDS uses a three-dimensional calculation approach, which must be performed within a domain of rectilinear volumes called meshes. When the model is being constructed, the quasi-space needs to be divided into many rectangular cells, and the simulation method of the cells is mainly separated into two types, uniform and non-uniform, as exhibited in Fig. 1 a and b. Considering the laws of conservation of energy, conservation of mass, and conservation of kinetic energy, each mesh is iteratively calculated and recalculated to produce relevant data, such as the possible temperature, smoke flow, air velocity, heat transfer, and particle movements, and so, each step is reliant on the physical properties of each cell [14].

FDS and SMV can run on all major 64-bit operating systems; however, the simulation software has relatively high computational demands, and systems attempting simulations should have at least 2–4 Gb RAM per IC core [15]. For this study, FDS 6.0 was used on a 3.1–4.0 GHz CPU, with 16 G Mb RAM.

FDS and SMV architecture

Three steps were involved in the process of FDS computation, as shown in Fig. 2. First, for the preprocessing stage, the parameters, such as fire settings and meshes, were specified in the input file. This was a name-list-formatted record. The purpose of doing so was to run the program in the next step. Second, the input file was used to produce an output for the data calculation. Next, as for the post-processing stage, the output of the data was visualized using 2D and 3D dynamics. Finally, the data were generated using SMV [16].
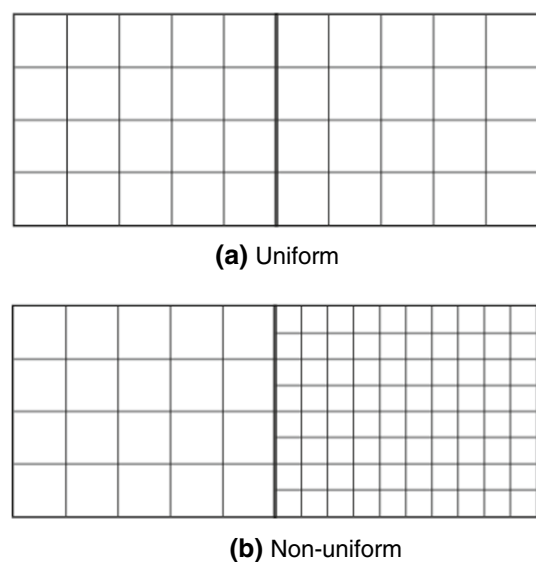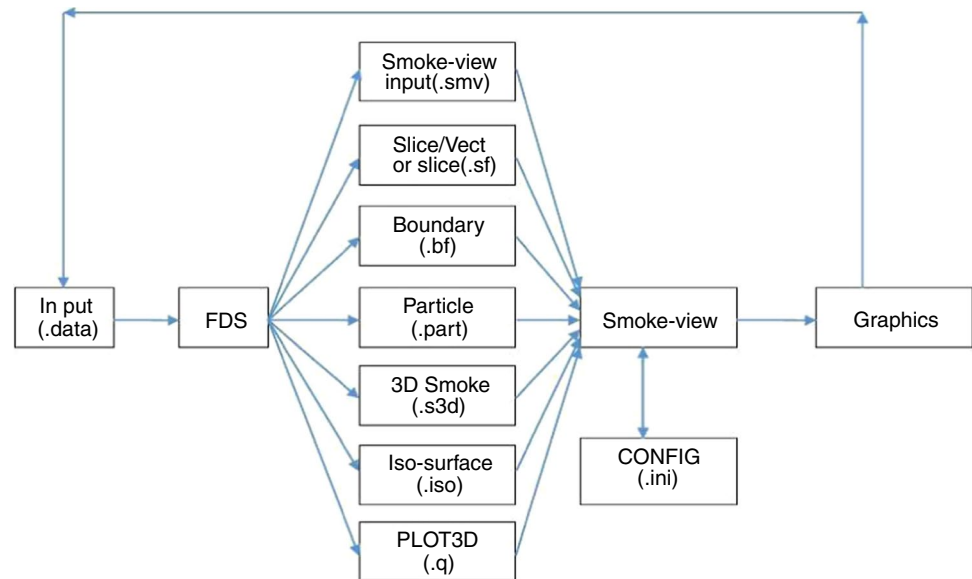

(a) Uniform

(b) Non-uniform

Fig. 1 Rules governing mesh alignment

Fig. 2 Architecture of FDS and SMV architecture

FDS setup

To better model a fire, the most commonly used approach is to describe the heat release rate during the growth stage, using t^2-fire. In this case, the heat release rate (HRR) is given by [17]:

$$\dot{Q} = \alpha t_0^2 \tag{1}$$

The reference heat release rate is usually taken to be 1055 kW and reflects the time taken to reach t_0 [18]. However, to improve the accuracy of the simulation results, the characteristic diameter D^* can be divided by the nominal size, δ_x, of a mesh cell, which should be between 4 and 16 [19]. Here the data should be closer to 16. The fire was suspected to have begun in the 34.0 cm gap between buildings A and B. The fire source parameter was set to 5000 kW m^{-2} for an adequate heat release rate of fire source, which is required to maintain the single-sided flame spread on a wooden board [20], and the fire source area was set to 0.6 m^2. This means the total heat release rate was 3000 kW, and the fire growth factor, α, was 0.188 kW s^{-2} [21]. Consequently, t_0 was computed via Eq. (1) and was determined to be 126.322 s. The mesh was designed with D^*, shown as Eq. (2), and following the FDS 6.0 user guide, Sect. 6.3.6 [19]:

$$D^* = \left(\frac{\dot{Q}}{\rho_\infty C_p T_\infty \sqrt{g}} \right) 2/5 \tag{2}$$

Meanwhile, four different nominal sizes, namely 0.05, 0.1, 0.2, and 0.25, were also tested in the simulation to find out the suitable simulation result when other parameter data were fixed.

The simulation material parameters also showed a noticeable effect on the FDS output. The wall of building A closest to the space was assigned as wood (yellow pine), and the wall of building B was designated as tile. The roofs of both buildings were appointed as iron. To better observe changes in temperature throughout the fire, thermocouples (THCPs) were set up at 0.9, 1.2, 1.5, 1.8, 2.1, and 2.4 m from the floor in building A, and 0.7, 1.0, 1.3, 1.6, 1.9, and 2.2 m from the floor in building B. These were assigned the codes A06–A01 and B06–B01, for buildings A and B, respectively. In addition, a slice was installed at $y = 270$ cm, where information about g the combustion, smoke flow, and temperature could be observed. The remaining parameter data used in this study are provided in Table 1.

Simulation results

After simulating with four different nominal sizes, results of the non-dimensional value are shown in Table 2 and the non-dimensional value 14.62 of the nominal size was the only one located between 4 and 16. Hence, the nominal size used in this research, which was 0.1, should be acceptable and reasonable [19]. Because all of the three dimensions were divisible into 0.1 m × 0.1 m × 0.1 m, and 20.0, 50.0, and 50.0, respectively, there were 50,000 mesh cells in total.

Figures 3 and 4 illustrate the gap between buildings A and B in SMV, where Fig. 3 represents the x-axis perspective and Fig. 4 the y-axis. The fire source was set between the buildings, and so, it is possible to see that building A is taller than building B. As described earlier, six thermocouples were positioned in each building at different heights.

Table 1 Use of FDS and SMV 3D parameters in this research

Model	Parameter	Contents	
Environmental fire	Ambient temperature/K, humidity/%, mesh/m	302.95	
		69	
		X: 2, Y: 5, Z: 5	
	OBST/m	X: 0.8–1.1	
		Y: 2.3–2.8	
		Z: 0.2–0.7	
	HRRPUA/kW m^{-2}	5000	
	TAU_Q/s	−126.322	
	SURF_ID	"INERT," "INERT," "frie," "frie," "frie," "frie"	
	Roof	IRON(NIST)	
	Specific heat/kJ [kg· K]$^{-1}$	0.44	
	Conductivity/W [m· K]$^{-1}$	80.4	
	Density/kg m^{-3}	7874.0	
	Wall of building A	Yellow pine (NIST)	
	Specific heat/kJ [kg· K]$^{-1}$	2.85	
	Conductivity/W [m· K]$^{-1}$	0.14	
	Density/kg m^{-3}	640.0	
	Heat of combustion/kJ kg^{-1}	0.0	
	Surface		
	Ignition temperature/°C	260.0	
	MATL_ID (1,1)	Yellow pine	
	HRRPUA/kW m^{-2}	1000 (default)	
	MATL_MASS_FRACTION (1,1)	1.0	
	Thickness (1)/m	0.005	
	Wall of building B	Tile (NIST)	
	Specific heat/kJ [kg· K]$^{-1}$	0.75	
	Conductivity/W [m· K]$^{-1}$	0.0611	
	Density/kg m^{-3}	313.0	
	Floor	Inert	
THCP	Building A	A01 (m)	X, Y, and Z=0.3, 2.2, and 2.4
		A02 (m)	X, Y, and Z=0.3, 2.2, and 2.1
		A03 (m)	X, Y, and Z=0.3, 2.2, and 1.8
		A04 (m)	X, Y, and Z=0.3, 2.2, and 1.5
		A05 (m)	X, Y, and Z=0.3, 2.2, and 1.2
		A06 (m)	X, Y, and Z=0.3, 2.2, and 0.9
	Building B	B01 (m)	X, Y, and Z=1.5, 2.2, and 2.2
		B02 (m)	X, Y, and Z=1.5, 2.2, and 1.9
		B03 (m)	X, Y, and Z=1.5, 2.2, and 1.6
		B04 (m)	X, Y, and Z=1.5, 2.2, and 1.3
		B05 (m)	X, Y, and Z=1.5, 2.2, and 1.0
		B06 (m)	X, Y, and Z=1.5, 2.2, and 0.7

Transient change of heat release rate (HRR)

In the simulation, Fig. 5 shows that the wooden wall of building A almost burned out entirely. In Fig. 6, the HRR of the initial fire source was 3000 kW. Although the HRR exceeded 12,000 kW because of the wooden wall in process, it returned and approached 3000 kW after 360 s. This shows a state of stable fire situation. The HRR time series plot and comparative chart are shown in Figs. 5 and 6, respectively.

Thermocouple data

Figures 7–13 present the temperatures recorded by the THCP setup in building A. The data obtained during the

Table 2 Results of the non-dimensional value

| Nominal sizes/δ_x	Non-dimensional value/$D^* \delta_x^{-1}$
0.05	29.24
0.1	14.62
0.2	7.31
0.25	5.85

180–600 s simulation were analyzed using probabilistic statistics. The statistical method of large sample confidence interval (CI) was used to do so, as this has already been proven reliable in the research into fire incidents. Because the standard deviation (σ) was unknown and displaced σ by standard deviation, the 100(1−α)% confidence interval for μ is given by Eq. (3):

$$\bar{x} - z_\alpha \frac{s}{\sqrt{n}} \leq \mu \leq \bar{x} + z_\alpha \frac{s}{\sqrt{n}} \tag{3}$$

When the sample size is greater than 40, Eq. (3) holds, regardless of the shape of the population distribution. Here, α is commonly assumed to be 0.05 for analysis purposes [22].

The data from the THCP A01 were calculated, the sample mean $\bar{x}$ was 156.07, the sample standard deviation s was 76.11, the sample size n was 701, and the α was 0.05. The CI of the THCP for A01 was $99.73 \leq \mu_{A01} \leq 212.41$. These steps were repeated for the remaining THCP data points, A02–A06, with the following results:

$$30.74 \leq \mu_{A02} \leq 86.91$$
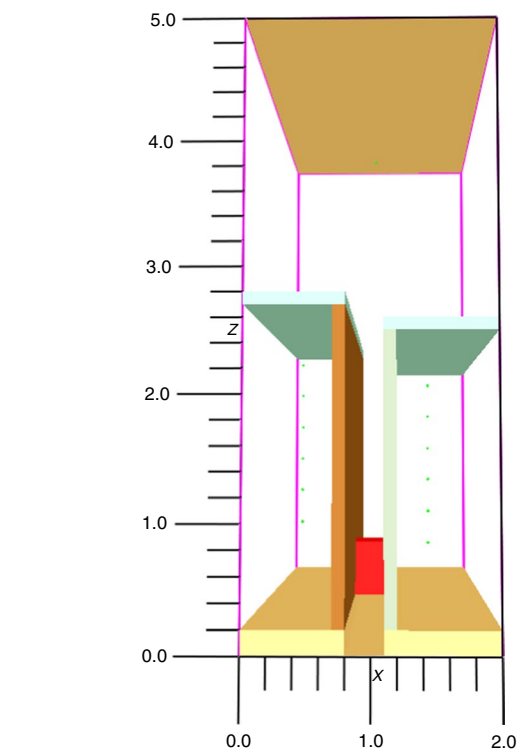
Fig. 4 Results of mesh size simulation presented in SMV; left: building A, right: building B

$$29.56 \leq \mu_{A03} \leq 65.67$$

$$30.35 \leq \mu_{A04} \leq 56.23$$

$$33.45 \leq \mu_{A05} \leq 46.68$$
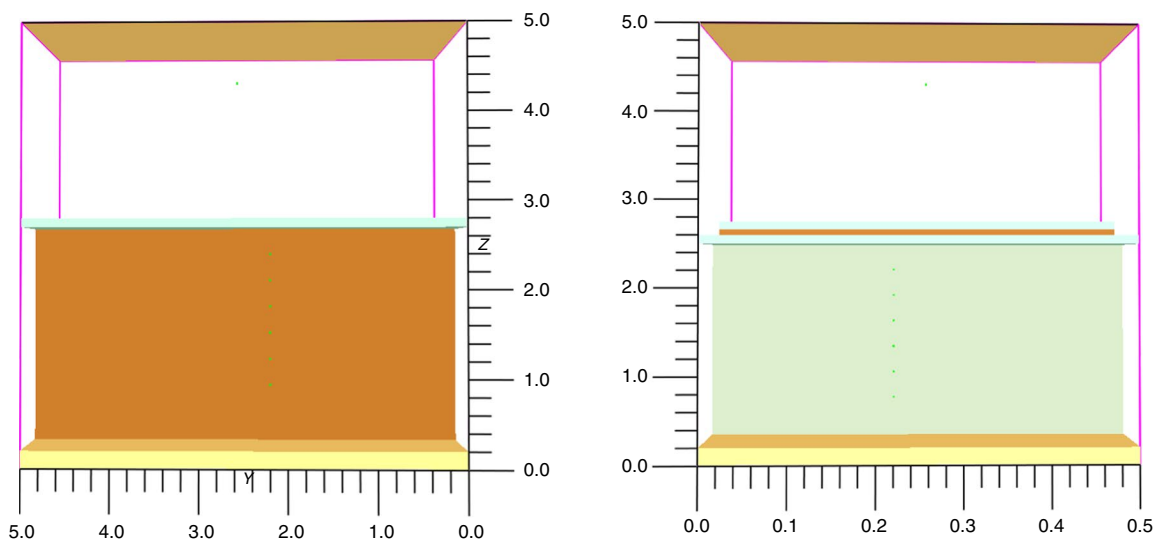
Fig. 3 Results of mesh size simulation presented in SMV; left side: building A, right side: building B

Fig. 5 Change of HRR over time for the space between buildings A and B
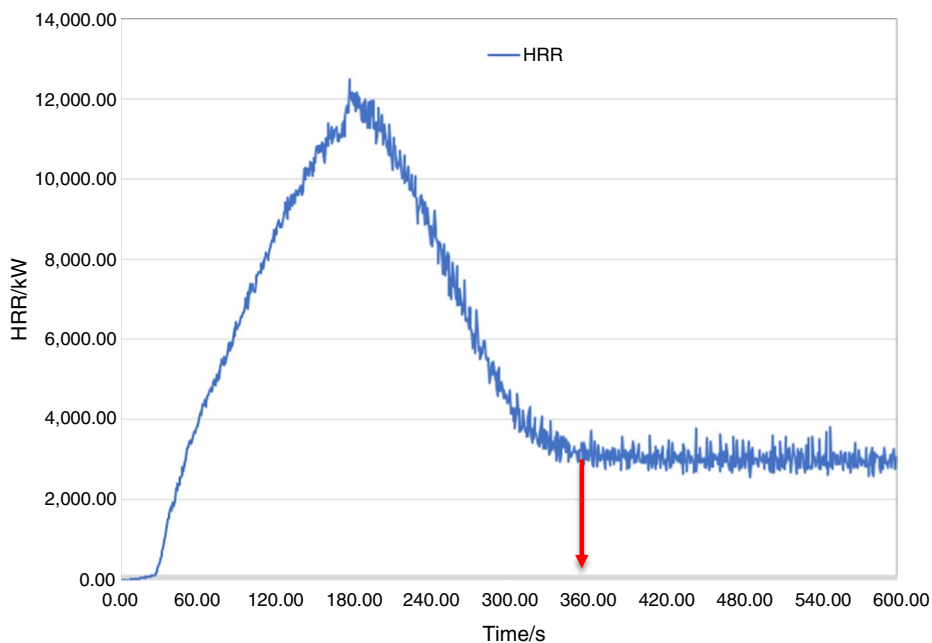
Fig. 6 SMV visualization of the fire in building A after 442 s
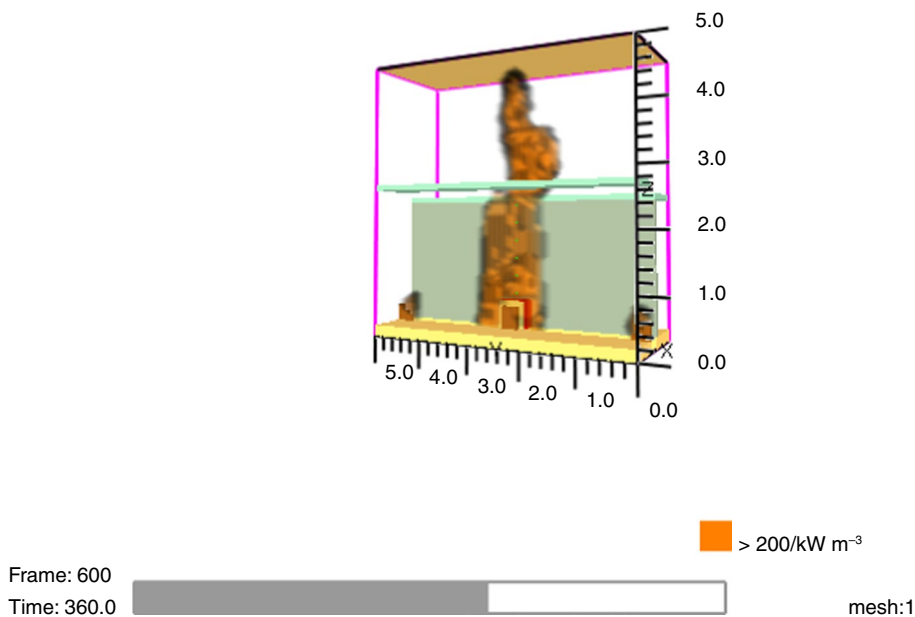
$$32.91 \leq \mu_{A06} \leq 44.30$$

Figure 13 shows a box-and-whisker plot of the data from THCP A01 to A06 with the relationship between the temperatures at these locations. As shown in Fig. 14, the temperatures obtained from the THCPs building B in stable combustion duration are described as follows: B01, B02, B03, B04, B05, and B06 were all 29.8 °C. Generally, temperatures from all of the six detection points in building A were higher than those in building B. The former also followed a pattern: The highest detection point detected the highest temperature in the six detections, and the lower detection point detected the lower temperature.

Comparative SMV findings from buildings A and B

Table 3 shows the images and information relating to combustion, the flow of smoke, and the temperature on the side of building A after 34.8, 170.4, 216, and 364.2 s. Table 3 also lists the images and information of combustion, the flow of smoke flow, and the temperature on the side of building B after the same time intervals.

Fig. 7 Gradual change of temperature with time in building A (THCP A01)
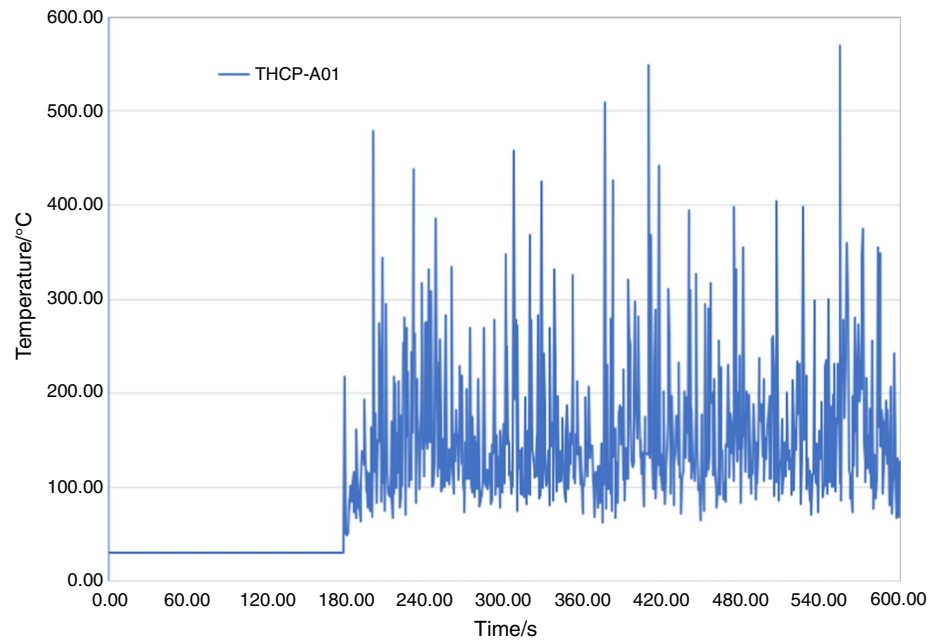
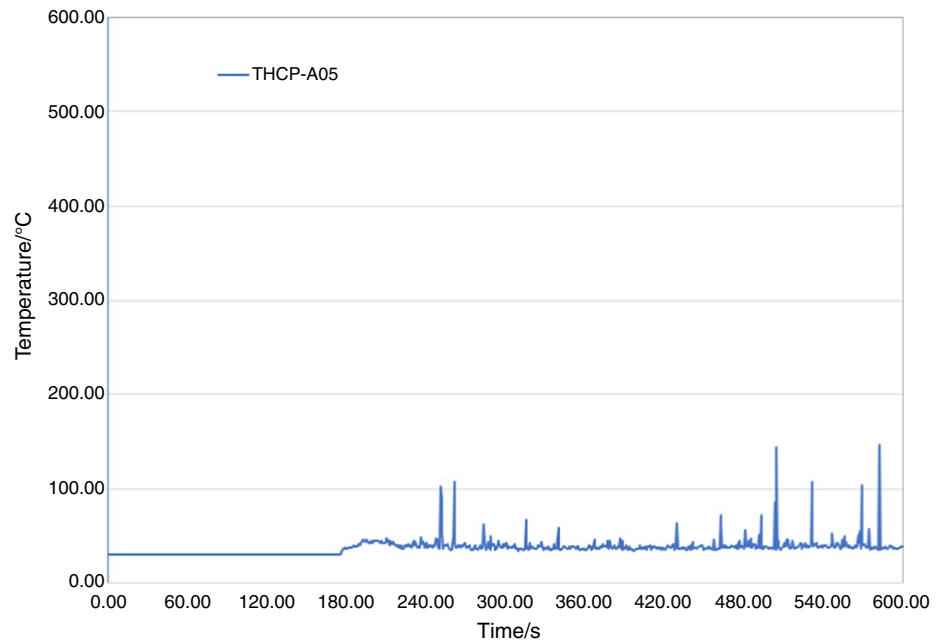**Fig. 8** Gradual change of temperature with time in building A (THCP A02)
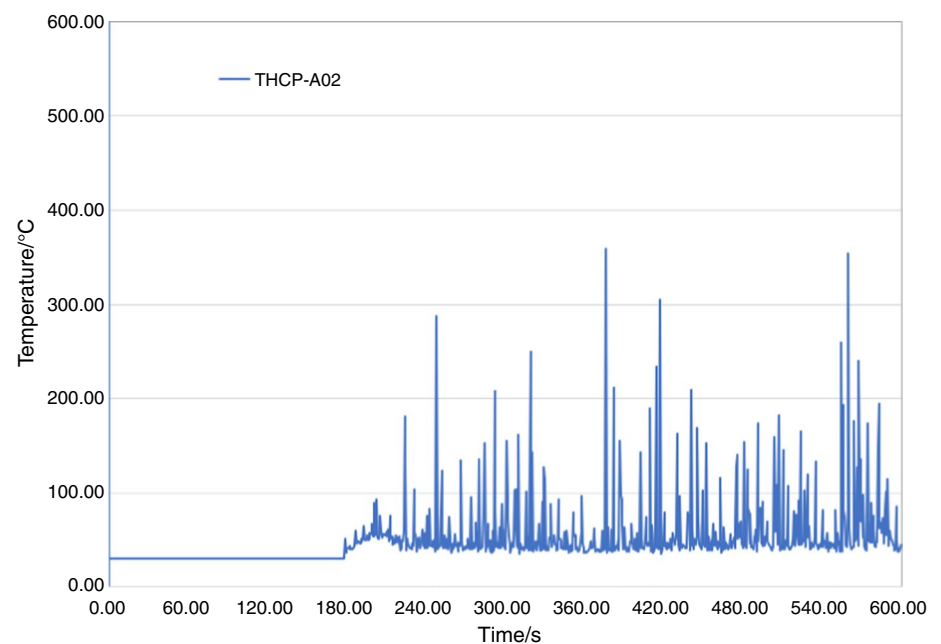
Building A: combustion and smoke flow

The fire source ignited in the gap between buildings A and B. The flow of heat appeared at 34.8 s, and immediately after this, the fire was giving off an immense amount of smoke in the space between the two buildings. After 170.4 s, there was no noticeable change in the walls of either building. At 216 s, roughly half of the wall of building A was burned down. At 364.2 s, the wall of building A was almost completely destroyed, and in the meantime, the smoke started to flow and enter building A.

Building B: combustion and smoke flow

Again, the fire source ignited in the gap between the buildings, and heat flow appeared around 34.8 s. Fire and smoke appeared in the space between the two buildings. After 170.4 s, there was no noticeable change in the walls of either

Fig. 9 Gradual change of temperature with time in building A (THCP A03)
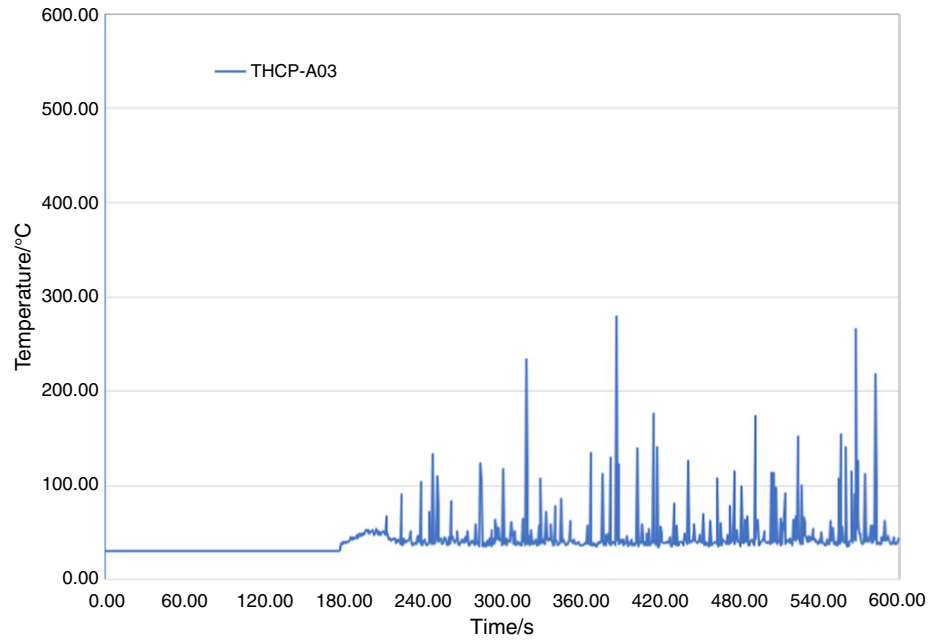
**Fig. 10** Gradual change of temperature with time in building A (THCP A04)
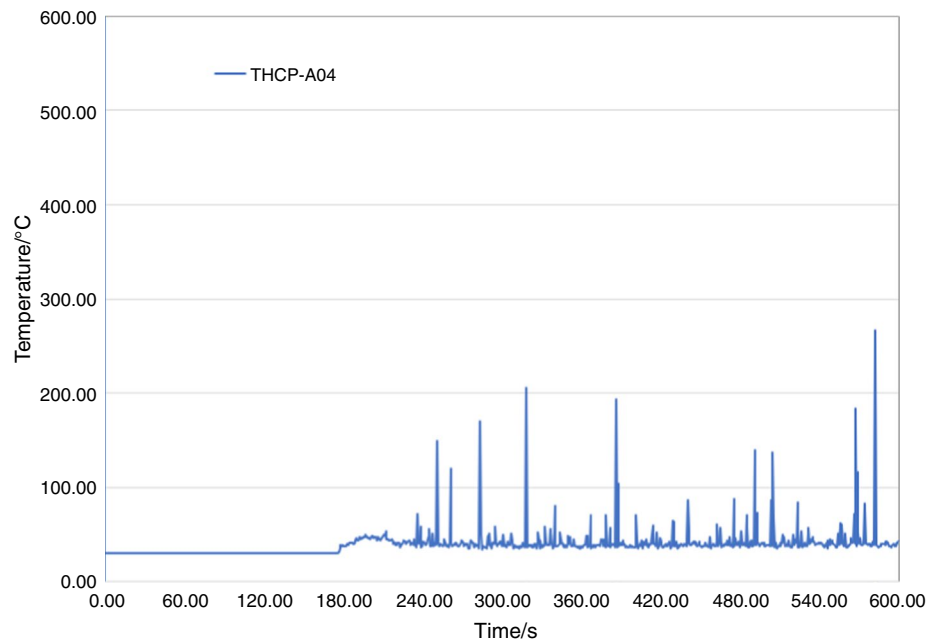
building. Even at 364.2 s, in the immediate presence of the fire, there was no visible effect on the wall of building B. No smoke flow had entered building B.

Results and discussion

The 2012 Chiayi City fire disaster tended to spread promptly and advanced through buildings because of the inherent disadvantage of the traditional style of wooden buildings. Building A was entirely built of wood, whereas the walls of building B of the second and third floors were made of asbestos shingles. At an elevation around the height of the second floor, there was a 34.0 cm gap between the buildings. In this simulation, the wall of building A was designated as a wooden structure, and the wall of building B was designated as a structure made of tiles. The simulated fire source was ignited in the space between buildings A and B. The parameters of the fire

Fig. 11 Gradual change of temperature with time in building A (THCP A05)

Fig. 12 Gradual change of temperature with time in building A (THCP A06)
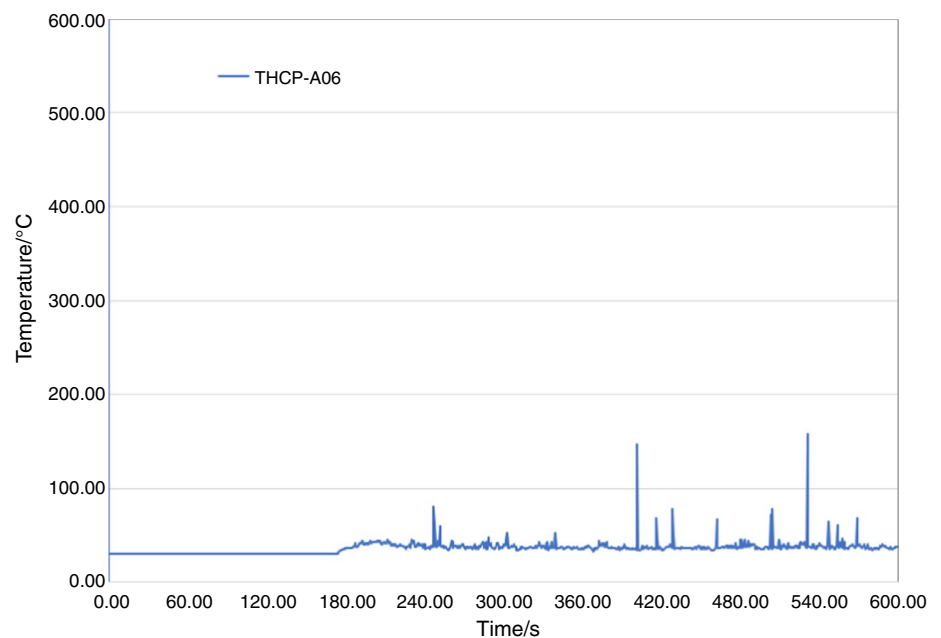
source, obstruction (OBST), mesh, and thermocouples used in this manuscript are presented in Table 1.

The simulation revealed the following information about the reconstructed scene and fire. Table 3 shows that roughly half of the wall of building A burned violently after 216 s. By 364.2 s, it was almost entirely burned down. Conversely, the wall of building B remained intact for the entire duration of the simulation. The destruction of the wooden wall in building A caused the smoke to flow into building A. Accordingly, the smoke was unable to flow and enter building B, as the wall remained intact.

Figures 7–12 show visualizations of the related spaces' smoke and heat flow conditions. This information was derived from a statistical analysis of the virtual THCPs. The THCPs were labeled A01–A06 for building A and B01–B06 for building B. Figure 13 shows the connection between the THCP temperatures in building A after 180 s. The statistical outliers were observed in all six THCPs in building A, including several extreme outliers. In some instances, the THCP A04 and A05 values were higher than those of THCP A01, because of the flow of heat and the characteristics of the fire's growth. The temperature of

Fig. 13 A box-and-whisker plots of the temperatures from THCPs A01–A06
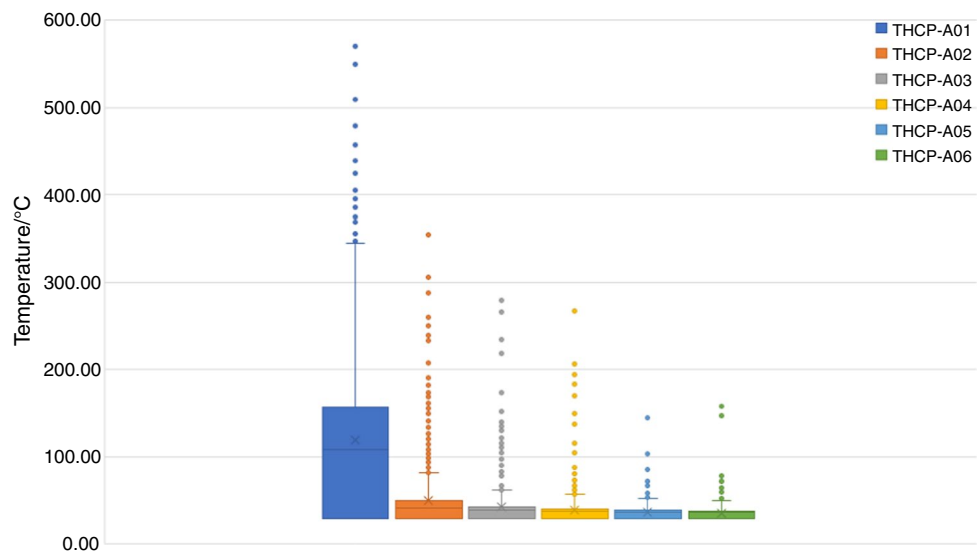
Fig. 14 Temperature variation *vs.* time from building B (THCPs B01–B06)
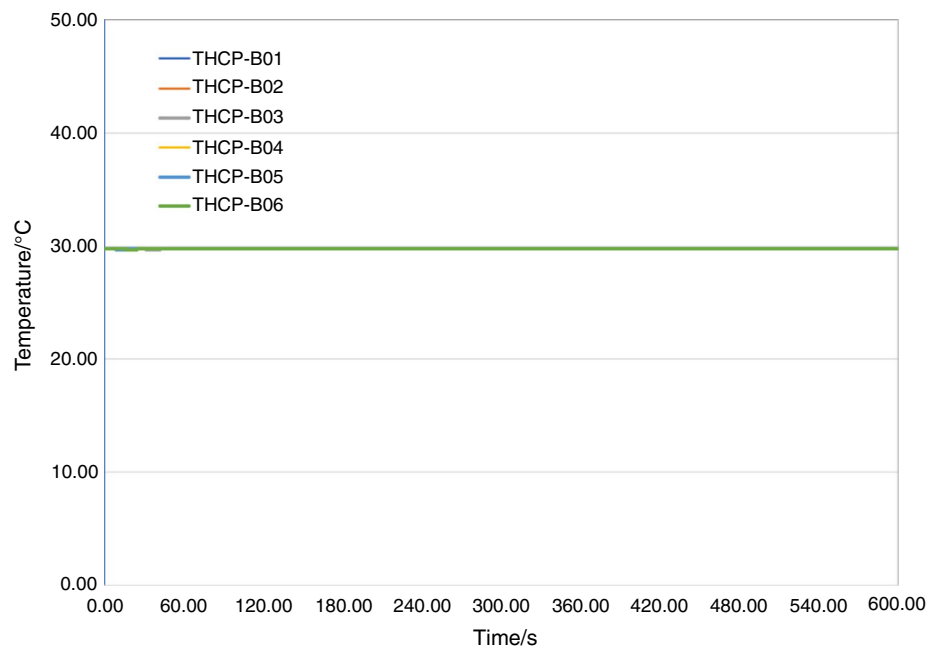
THCP A01 was higher than any other value, the temperature of THCP A02 was higher than the rest of the values, and so on.
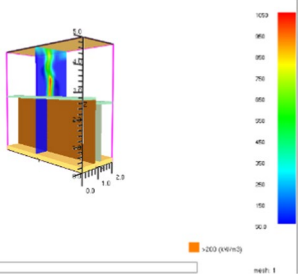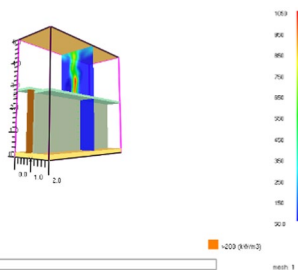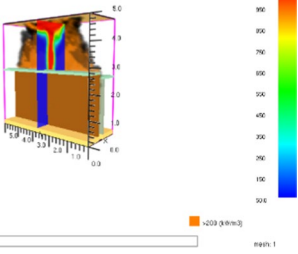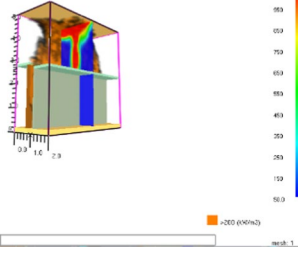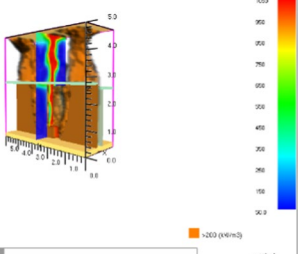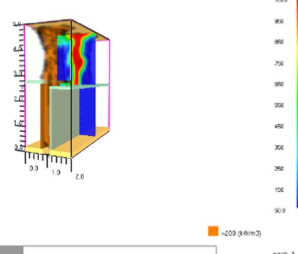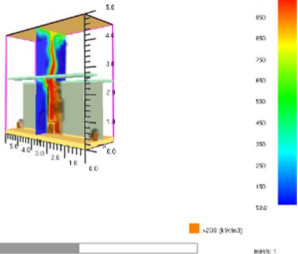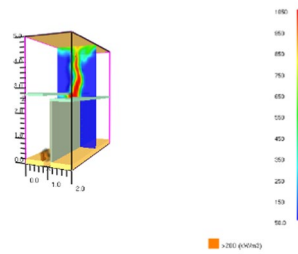
Figures 7–12 show that the temperature rise line was almost straight for the first 180 s, but increased afterward. This change might have been because the advance of the smoke and fire was retarded by the outer wall of building A until it collapsed. This means that the temperatures recorded by the THCPs remained ambient for some time.

The THCP temperatures in building B during the stable combustion period remained around 29.8 °C, as shown in Fig. 14. This suggests that no smoke or fire could enter building B.

After comparing the THCP temperatures from the two buildings, the temperatures at the six detection points in building A were higher than those in building B. Furthermore, the higher the temperatures in building A, the greater their elevation, which can be seen in the temperature–time charts provided in Figs. 7–12.

Some events may have occurred, but the simulation did not detect them. For instance, tiles might have been destroyed after long-term exposure to high temperatures, for this could have allowed smoke and fire to enter building B; however, as it stands, the proposed model validates the suspected causes of the fire and the observed damage.

Table 3 Simulated combustion output for buildings A and B after specific time duration

	Building A	Building B
Duration (s)	34.8	
Combustion configuration		
Duration (s)	170.4	
Combustion configuration		
Duration (s)	216	
Combustion configuration		
Duration (s)	364.2	
Combustion configuration		

In addition, it corroborates the available resident and witness statements.

Some confounding elements are provided as follows. Residents and witnesses saw the smoke disappearing from the upper floor of building B, and they heard the sound of an explosion from the direction of building B. However, neither smoke nor fire was observed in building A during the initial period. The CCTV equipment in building A also shows no signs of fire or smoke on the second floor or the stairway of building A.

If the fire had started to burn in the space between buildings A and B, the details given by the witnesses would have described the smoke coming from building A instead of building B, or at the very least they would have characterized the smoke coming from both buildings. For example, the tiles had been destroyed after their long-term

exposure to high temperatures. Consequently, it is reasonable that these fire investigators excluded the possibility of how the fire commenced to burn in the space between buildings A and B.

Conclusions

Initially, fire investigators' speculation about the event did not include the possibility of whether the fire started to burn in the space between the two buildings. This speculation assumed that it should have burned among the buildings somewhat equally, images of CCTV, and statements of the witnesses.

Based on the results obtained from the simulation, if the fire had started at the interval between buildings A and B, the smoke that witnesses saw should not have traveled from the upper floor of building B. Therefore, based on the results obtained from the simulation, it was reasonable for the fire investigators to exclude the fact that the fire had started at the interval between buildings A and B.

However, caution should be paid to other possibilities, such as the complete damage of tiles caused by long-term exposure to high temperature, the wind direction, the internal structure of the buildings, and any other factors that could affect the fire route and the smoke flow. As mentioned, the other possibilities can be researched in the future. Furthermore, the fire source can be set to different ignition sources, such as high-temperature objects, sparks, or cigarette butts, to confirm whether it will cause different results. Meanwhile, other investigators can apply the scientific methods under strict conditions in their investigation in Taiwan.

Declarations

References

1. Laboratory FP. Wood Handbook-Wood as an Engineering Material, General Technical Report FPL-GTR-190. Forest Service, Forest Products Laboratory, Madison, WI, USA: U.S. Department of Agriculture; 2010.

2. Hu HW, Shi JG, Qi ZY, Ji J. Experimental investigations on transient burning characteristics of a butt-jointed wooden wall with horizontal gaps in timber buildings. State Key Laboratory of Fire Science: University of Science and Technology of China, Hefei, Anhui, China; 2023.

3. Torero J. Flaming ignition of solid fuels, in: SFPE Handb. Fire Prot. Eng., 5th ed., Springer New York Heidelberg Dordrecht London, London, UK, 2016;633–661.

4. Drysdale D. An Introduction to Fire Dynamics, 3rd ed., John Wiley & Sons, Ltd., Edinburgh, Scotland, UK, 2011. https://doi.org/10.1016/0010-2180(86)90037-4.

5. Karlsson B, Quintiere JG. Enclosure Fire Dynamics. 1st ed. Boca Raton, FL, USA: CRC Press; 1999.

6. Li K, Hostikka S, Dai P, Li Y, Zhang H, Ji J. Charring shrinkage and cracking of fir during pyrolysis in an inert atmosphere and at different ambient pressures. Proc Combust Inst. 2017;36:3185–94. https://doi.org/10.1016/j.proci.2016.07.001.

7. Ferrantelli A, Baroudi D, Khakalo S, Li KY. Thermomechanical surface instability at the origin of surface fissure patterns on heated circular MDF samples. Fire Mater. 2019;43:707–16. https://doi.org/10.1002/fam.2722.

8. Baroudi D, Ferrantelli A, Li KY, Hostikka S. A thermomechanical explanation for the topology of crack patterns observed on the surface of charred wood and particle fibreboard. Combust Flame. 2017;182:206–15. https://doi.org/10.1016/j.combustflame.2017.04.017.

9. Wang S, Ding P, Lin S, Huang X, Usmani A. Deformation of wood slice in fire: interactions between heterogeneous chemistry and thermomechanical stress. Proceed Combust Inst. 2021;38:5081–90. https://doi.org/10.1016/j.proci.2020.08.060.

10. Wei PE, Long-hua HU, Rui-xin YA, Qing-feng LV, Fei TA, Yong XU, Li-yuan W. Full scale test on fire spread and control of wooden buildings. Proced Eng. 2011;1(11):355–9.

11. NFPA 921: Guide for fire and explosion investigations, 2011 ed., Quincy, Massachusetts, USA.

12. DeHaan JD, Icove DJ. Kirk's Fire Investigation. 7th ed. Julie Levin Alexander, London, England: Pearson Education Press; 2012.

13. Fire report of Fire Bureau, Chiayi City Government Fire report. Chiayi, Taiwan, ROC, 2012.

14. McGrattan K, McDermott R, Vanella M, Hostikka S, Floyd J, Fire dynamics simulator technical reference guide, National Institute of Standards and Technology, Maryland, Gaithersburg, USA, NIST Special Publication 1018, 2013a.

15. McGrattan K, McDermott R, Vanella M, Hostikka S, Floyd J, Fire dynamics simulator user's guide, National Institute of Standards and Technology, Maryland, Gaithersburg, USA, NIST Special Publication 1019, 2013b.

16. Forney GP. Smokeview (version 6)—A tool for visualizing fire dynamics simulation data volume I: User's guide, national institute of standards and technology, Gaithersburg, Maryland, USA, NIST Special Publication 1017–1, 2013.

17. Hurley MJ, Rosenbaum ER. Performance-Based Fire Safety Design. Boca Raton, Florida, USA: CRC Press; 2015.

18. Staffansson L. Selecting design fires. Department of Fire Safety Engineering and Systems Safety: Lund University, Lund, Scania, Swedish; 2010.

19. McGrattan K, McDermott R, Weinschenk C, Overholt K, Hostikka S, Floyd J. NIST Special Publication 1019 Fire Dynamics Simulator User's Guide Version 6, National Institute of Standards and Technology, Gaithersburg, Maryland, USA, 2014.

20. Hakkarainen T, Oksanen T. Fire safety assessment of wooden facades. Fire Mater. 2002;26:7–27. https://doi.org/10.1002/fam.780.

21. Karlsson B, Quintiere GJ. Enclosure fire dynamics. Boca Raton, Florida, USA: CRC Press; 2000.
22. Montgomery DC, Runger GC. Applied Statistics and Probability for Engineers. 6th ed. International Student Version: Arizona State University, Tempe, Arizona, USA; 2014.